NASA Technical Memorandum 84657

Inviscid Analysis of Two Supercritical Laminar-Flow-Control Airfoils at Design and Off-Design Conditions

Dennis O. Allison

JUNE 1983

25th Anniversary
1958-1983

NASA

NASA Technical Memorandum 84657

Inviscid Analysis of Two Supercritical Laminar-Flow-Control Airfoils at Design and Off-Design Conditions

Dennis O. Allison
Langley Research Center
Hampton, Virginia

National Aeronautics
and Space Administration

**Scientific and Technical
Information Branch**

1983

SUMMARY

Inviscid transonic flow results are presented for two supercritical laminar-flow-control airfoils in such a way that they can be compared at design and off-design Mach numbers and lift coefficients. Two-dimensional design Mach numbers for the two airfoils are 0.755 and 0.730 at a common design lift coefficient of 0.60, and thickness-to-chord ratios are 0.131 and 0.135, respectively. Results are presented for Mach numbers between 0.6 and 0.8 and lift coefficients from 0.4 to 0.7.

The newer airfoil, with its lower suction requirements for full-chord laminar flow, has a higher design Mach number, steeper pressure gradients, a more positive pressure level in the forward region of the lower surface, and a recovery to a less positive pressure at the trailing edge. Off-design shock-formation characteristics are similar for the two airfoils even though the respective design Mach numbers are quite different. The newer airfoil is similar to the one used in a large-chord swept-model experiment designed for the Langley 8-Foot Transonic Pressure Tunnel.

INTRODUCTION

Laminar-flow-control (LFC) application has gained new interest (ref. 1) based on the following: the success of previous programs in achieving drag reduction through laminar flow, large potential fuel savings coupled with high fuel prices, developments in materials and fabrication, and advances in airfoil technology. One of the newest advances in LFC airfoil design involves supercritical technology. Recently, a complex laminar-flow-control experiment using supercritical technology was designed for the Langley 8-Foot Transonic Pressure Tunnel (refs. 2 to 7). This LFC experiment simulates flow around an infinite-span swept airfoil at transonic speeds and requires a low-turbulence wind tunnel (refs. 4 and 7) with nonporous contouring (refs. 3 and 6) of all four walls to minimize flow interference around the large-chord model. Many iterations involving airfoil shape, suction distribution, sweep angle, wall contouring, and other variables were required to design this experiment. Two representative airfoil shapes are considered in the present analysis. They are referred to hereafter as airfoil A and airfoil B. Airfoil B is similar to the final airfoil for the complex LFC experiment (ref. 7). Airfoil A, referred to as LFC-73-06-135 in reference 2, was designed for a leading-edge sweep of 35° and a free-stream Mach number of 0.891. Airfoil B, referred to as 989C in reference 5, was designed for a reduced leading-edge sweep of 23° and a free-stream Mach number of 0.820.

The term "design condition" in the present paper refers to a maximum two-dimensional Mach number at a given lift coefficient for which no incipient shock wave exists in the pressure distribution. For an LFC airfoil, this design Mach number is of particular interest, since an incipient shock wave could either require additional suction or cause transition to turbulent flow. This design Mach number occurs just below drag divergence and, for a lift coefficient of 0.60, is 0.730 for airfoil A and 0.755 for airfoil B. A higher design Mach number leads to a lower sweep angle, which reduces the problems from leading-edge contamination (spread of the turbulent boundary layer along the flow attachment line) and crossflow instability. The design philosophy of airfoils A and B has been discussed previously in references 2 and 5. A high design Mach number and full-chord laminar flow with low suction requirements were two primary goals. Another important goal was to avoid shock-wave formation at

Mach numbers and lift coefficients below design and to avoid strong shocks at a given Mach number or lift coefficient increment above design. The pressure distributions for airfoils A and B are characterized by alternate regions of steep and shallow pressure gradients. This is true because the crossflow instability dominates in regions of steep pressure gradients but depends more on chordwise extent than steepness of gradients. Control of the crossflow instability requires much more suction (ref. 8) than control of the Tollmien-Schlichting instability, which dominates in regions of small pressure gradients. Suction requirements are therefore reduced by confining steep pressure gradients to shorter distances (making them steeper) while extending small gradients over longer distances. However, this philosophy forces the steep adverse pressure gradients to become more difficult to tailor for control of flow separation. Laminar-boundary-layer disturbance growth factors and LFC suction requirements, which have been analyzed previously for the two airfoils, are defined and discussed with emphasis on the crossflow instability in references 2, 5, and 8.

The purpose of the present paper is to document inviscid pressure distributions, pitching-moment coefficients, and wave drag coefficients at design and off-design flow conditions in such a way that they can be compared for airfoils A and B. The comparison has benefit for the design of future LFC airfoils involving supercritical technology. Inviscid transonic flow results, computed by the two-dimensional method of reference 9 (with corrected wave drag, ref. 10), are used to compare pressure levels and gradients as well as shock-wave formation for the two supercritical laminar-flow-control airfoils. Inviscid (no boundary layer) results are used under the assumption that the full-chord laminar boundary layer will be kept thin by suction. Results are presented for Mach numbers between 0.6 and 0.8 and lift coefficients from 0.4 to 0.7.

SYMBOLS

All parameters listed below correspond to two-dimensional airfoil characteristics.

$c_{d,w}$ section wave drag coefficient

c_l section lift coefficient

c_m section pitching-moment coefficient about the quarter-chord point

C_p pressure coefficient

M Mach number

M_{DD} drag-divergence Mach number

t/c thickness-to-chord ratio

x/c distance measured along chord divided by chord

Abbreviation:

LFC laminar flow control

RESULTS AND DISCUSSION

Inviscid transonic flow results at design and off-design Mach numbers and lift coefficients are presented for airfoils A and B. Airfoil geometry is presented in figure 1; geometry variations such as flap deflections are not considered. As noted in figure 1, the thickness-to-chord ratios for airfoils A and B are 0.135 and 0.131, respectively. Geometric differences between airfoils A and B are discussed as their significance is revealed through comparisons of pressure distributions. As explained in the "Introduction," all results are computed with no boundary layer by the method of references 9 and 10. These results consist of surface pressure distributions, shapes of supersonic flow regions, pitching-moment coefficients, and wave drag coefficients for $M = 0.6$ to $M = 0.8$ and $c_l = 0.4$ to $c_l = 0.7$. A comparison of pressure distributions for low Mach numbers is given in figures 2 and 3, and design conditions are discussed with reference to figures 2 through 5. A wave drag comparison is shown in figure 6, characteristics of design pressure distributions for $c_l = 0.6$ are shown in figure 7, and shock-formation characteristics at off-design conditions are discussed with reference to figures 8 through 13.

Both airfoils exhibit a negative leading-edge pressure peak at $M = 0.600$, $c_l = 0.60$ (figs. 2(a) and 3(a)). Such a peak exists at lower Mach numbers and higher lift coefficients but diminishes at higher Mach numbers (figs. 2 and 3). Since airfoil B has a smaller leading-edge radius (fig. 1), it has a more negative leading-edge pressure peak (fig. 3(a)) than airfoil A (fig. 2(a)), and it is more susceptible to forward boundary-layer separation without a leading-edge device. The more negative leading-edge pressure peak and higher pressure level in the first 20 percent of the lower surface are, of course, caused by geometric differences in the leading edge and carved-out lower surface region of airfoil B compared with airfoil A (fig. 1). A device could be designed for storage in the first 20 percent of chord of the lower surface (refs. 5 and 11) where airfoil B has a lower local velocity (higher pressure level in fig. 3(a) compared with that for airfoil A in fig. 2(a)). The lower velocity, which is more conducive to laminar flow without suction, means that a joint in the surface is less likely to cause transition to turbulent flow.

For comparisons of aerodynamic characteristics, the design conditions for airfoils A and B are defined after a few comments concerning other similar conditions. The condition of $M = 0.755$, $c_l = 0.55$ was selected for the LFC airfoil experiment at the Langley Research Center, while airfoil B was conceived for the condition of $M = 0.758$, $c_l = 0.58$ (refs. 5 and 7). The smooth pressure distributions in figures 5(a) and 5(b) for these two conditions indicate the absence of shock waves. As Mach number and lift coefficient are increased for airfoil B (figs. 5(c) and 5(d)), a shock wave is indicated by the pressure distributions. A design condition in the present paper is taken, for a given lift coefficient, as a maximum Mach number for which no incipient shock wave, such as that in figure 5(c), has formed. An incipient shock wave is a disturbance in the pressure distribution, such as that in figure 5(c) at about 70 percent of chord on the upper surface, which develops into a shock wave for slightly higher Mach numbers and/or lift coefficients (see fig. 5(d)). For airfoil A, similar cases are presented in figure 4, where the Mach number is 0.025 lower than for airfoil B (fig. 5) in each case. For a constant section lift coefficient of 0.60, pressure distributions for small increases in Mach number are shown in figures 2(c), 4(c), and 8(c) for airfoil A and in figures 3(d), 5(c), and 9(c) for airfoil B. For airfoils A and B, incipient shock waves form for $M = 0.735$ and $M = 0.760$, respectively; therefore, the respective design Mach numbers are 0.730 and 0.755. Note that the wave drag coefficient is zero at the design condition of each airfoil (figs. 2(c) and 3(d)).

The wave drag coefficient increases through drag divergence as Mach number is increased (fig. 6). The drag-divergence Mach numbers M_{DD}, or Mach numbers at which $dc_{d,w}/dM = 0.1$, are 0.755 and 0.775 for airfoils A and B, respectively. Drag divergence occurs at a Mach number of 0.025 above design for airfoil A and similarly at 0.020 above design for airfoil B.

Pressure distributions are compared for the two airfoils at their respective design conditions in figure 7. In contrast to the favorable pressure gradient on the upper surface of a low-speed natural-laminar-flow airfoil, the small upper-surface pressure gradient is adverse for airfoils A and B as dictated by supercritical technology. For airfoil B, the greater extent of supersonic flow on the upper surface (about 80 percent of chord compared with about 65 percent of chord for airfoil A) results from the more nearly flat geometry of the upper surface (fig. 1). Each pressure gradient (fig. 7) on the upper or lower surface of airfoil B which is steeper than the corresponding one for airfoil A results from a region of higher curvature (fig. 1). As explained in the "Introduction," these steeper gradients reduce the suction requirements for control of the crossflow instability. Also, the less positive base pressure (fig. 7), which shortens the pressure recovery to the trailing edge for airfoil B compared with airfoil A, results from the smaller angle between the upper and lower surfaces at the trailing edge (fig. 1). It is interesting to note that the front and rear lower-surface concave regions for both airfoils (fig. 1) could be geometrically refined to include one or more corners (quick turns joined by straight lines) in an attempt to control the Taylor-Goertler instability (ref. 5). However, the treatment of such refinements is beyond the scope of the present analysis.

Experience with the redesign of an airfoil for a higher Mach number leads one to check for the formation of a shock wave for Mach numbers or lift coefficients below design or a strong shock wave for a given Mach number or lift coefficient increment above design even if this does not occur for the airfoil with the lower design Mach number. Airfoils A and B show similar shock-formation behavior for increments of 0.015 in Mach number below and above their respective design conditions (figs. 8 and 9). The two airfoils are free from lower-surface shocks at $c_l = 0.40$ and have similar upper-surface shocks at $c_l = 0.70$ for their respective design Mach numbers (figs. 10 and 11). For $c_l = 0.70$, the two airfoils show similar development and movement of upper-surface shock waves for $M = 0.600$ and higher (figs. 12 and 13).

CONCLUDING REMARKS

Inviscid transonic flow results are provided for two supercritical laminar-flow-control airfoils. Airfoil A has the advantage of a less negative leading-edge pressure peak at Mach numbers of 0.6 and lower. Airfoil B makes use of steeper pressure gradients on the upper and lower surfaces to reduce boundary-layer suction requirements. The first 20 percent of chord of the lower surface of airfoil B provides a more positive pressure level, which is more conducive to laminar flow with no suction. The less positive trailing-edge pressure for airfoil B compared with that for airfoil A shortens the pressure recovery to the trailing edge. The thickness-to-chord ratios are about the same for the two airfoils (0.131 for airfoil B and 0.135 for airfoil A). Airfoil B has the important advantage of a higher design Mach number than airfoil A (0.755 compared with 0.730 at a lift coefficient of 0.60). Nevertheless, off-design shock-formation characteristics are similar for the two airfoils

over a range of Mach numbers between 0.6 and 0.8 and lift coefficients from 0.4 to 0.7. Based on these results, airfoil B has better potential than airfoil A for application of supercritical technology to a swept laminar-flow-control wing.

Langley Research Center
National Aeronautics and Space Administration
Hampton, VA 23665
April 25, 1983

REFERENCES

1. Wagner, Richard D.; and Fischer, Michael C.: Developments in the NASA Transport Aircraft Laminar Flow Program. AIAA-83-0090, Jan. 1983.

2. Allison, Dennis O.; and Dagenhart, John R.: Design of a Laminar-Flow-Control Supercritical Airfoil for a Swept Wing. CTOL Transport Technology - 1978, NASA CP-2036, Pt. I, 1978, pp. 395-408.

3. Newman, Perry A.; and Anderson, E. Clay: Analytical Design of a Contoured Wind-Tunnel Liner for Supercritical Testing. Advanced Technology Airfoil Research, Volume I, NASA CP-2045, Pt. 2, 1979, pp. 499-509.

4. Bobbitt, Percy J.: Modern Fluid Dynamics of Subsonic and Transonic Flight. AIAA-80-0861, May 1980.

5. Pfenninger, W.; Reed, Helen L.; and Dagenhart, J. R.: Design Considerations of Advanced Supercritical Low Drag Suction Airfoils. Viscous Flow Drag Reduction, Gary R. Hough, ed., AIAA, c.1980, pp. 249-271.

6. Newman, Perry A.; Anderson, E. Clay; and Peterson, John B., Jr.: Numerical Design of the Contoured Wind-Tunnel Liner for the NASA Swept-Wing LFC Test. AIAA-82-0568, Mar. 1982.

7. Harvey, W. D.; and Pride, J. D.: The NASA Langley Laminar Flow Control Airfoil Experiment. AIAA-82-0567, Mar. 1982.

8. Dagenhart, J. Ray: Amplified Crossflow Disturbances in the Laminar Boundary Layer on Swept Wings With Suction. NASA TP-1902, 1981.

9. Bauer, Frances; Garabedian, Paul; Korn, David; and Jameson, Antony: Supercritical Wing Sections II. Volume 108 of Lecture Notes in Economics and Mathematical Systems, Springer-Verlag, 1975.

10. Bauer, Frances; Garabedian, Paul; and Korn, David: Supercritical Wing Sections III. Volume 150 of Lecture Notes in Economics and Mathematical Systems, Springer-Verlag, 1977.

11. Applin, Zachary T.: Status of NASA Advanced LFC Airfoil High-Lift Study. Laminar Flow Control - 1981 Research and Technology Studies, NASA CP-2218, 1982, pp. 43-61.

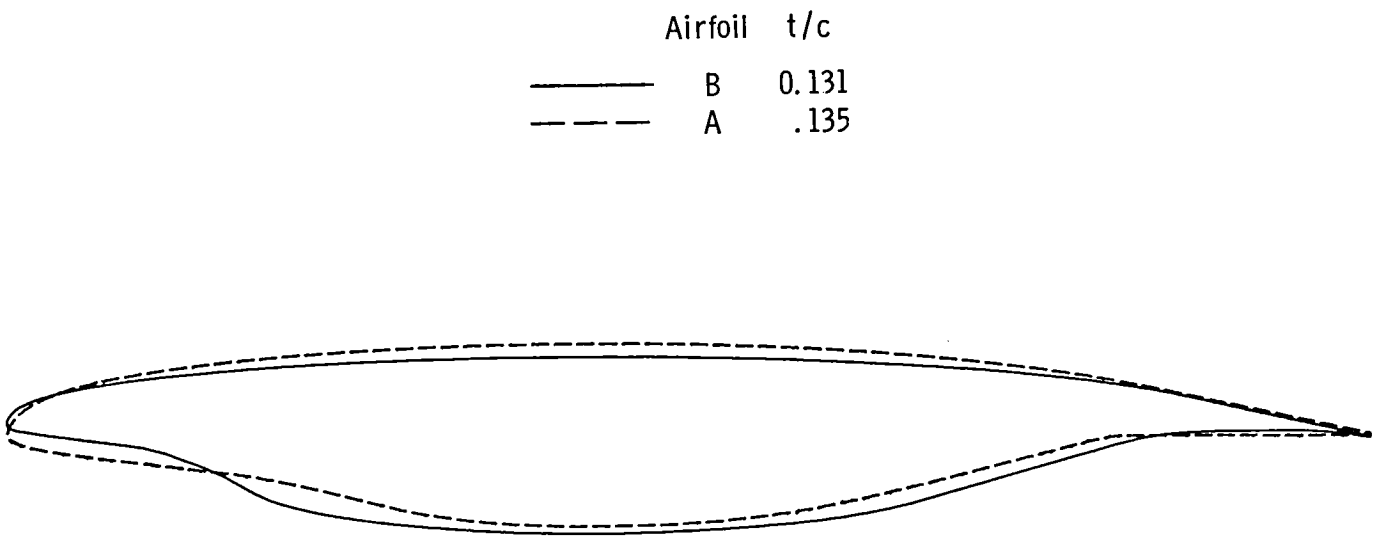

Figure 1.- Comparison of geometry for the two airfoil concepts.

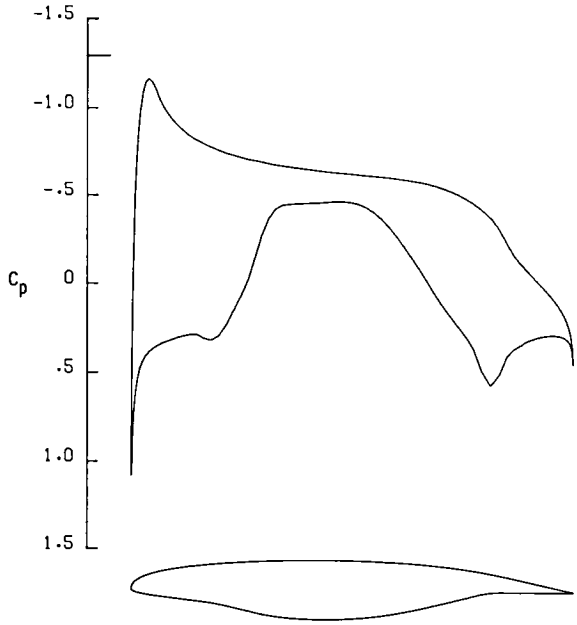

(a) M = 0.600; c_m = -0.086; $c_{d,w}$ = 0.0000.

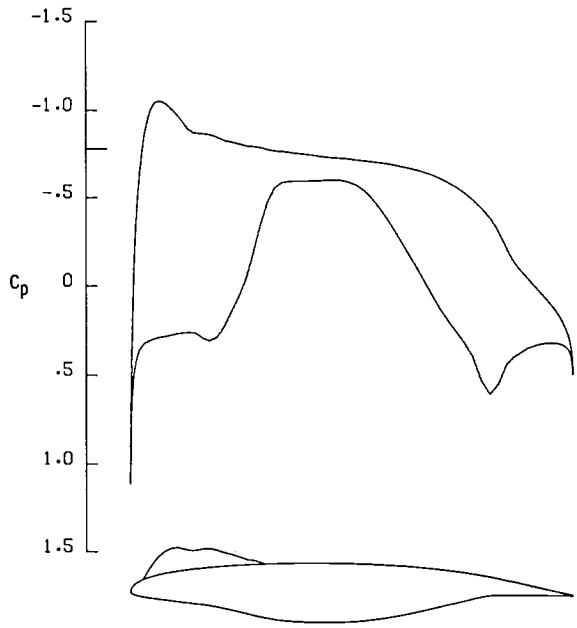

(b) M = 0.700; c_m = -0.098; $c_{d,w}$ = 0.0000.

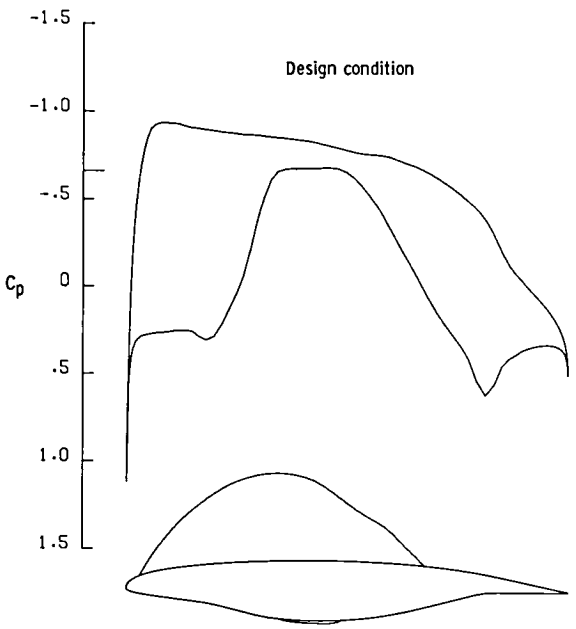

(c) M = 0.730; c_m = -0.104; $c_{d,w}$ = 0.0000.

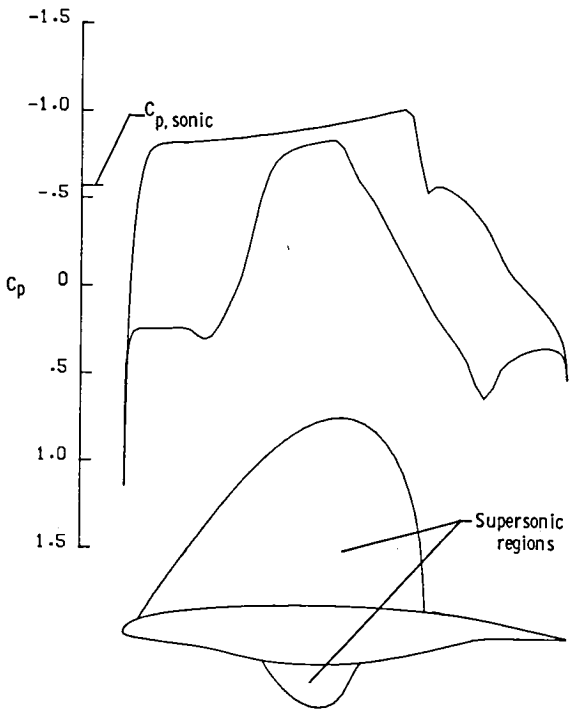

(d) M = 0.755; c_m = -0.119; $c_{d,w}$ = 0.0010.

Figure 2.- Pressure distributions for airfoil A at M = 0.600 to M = 0.755. c_l = 0.60.

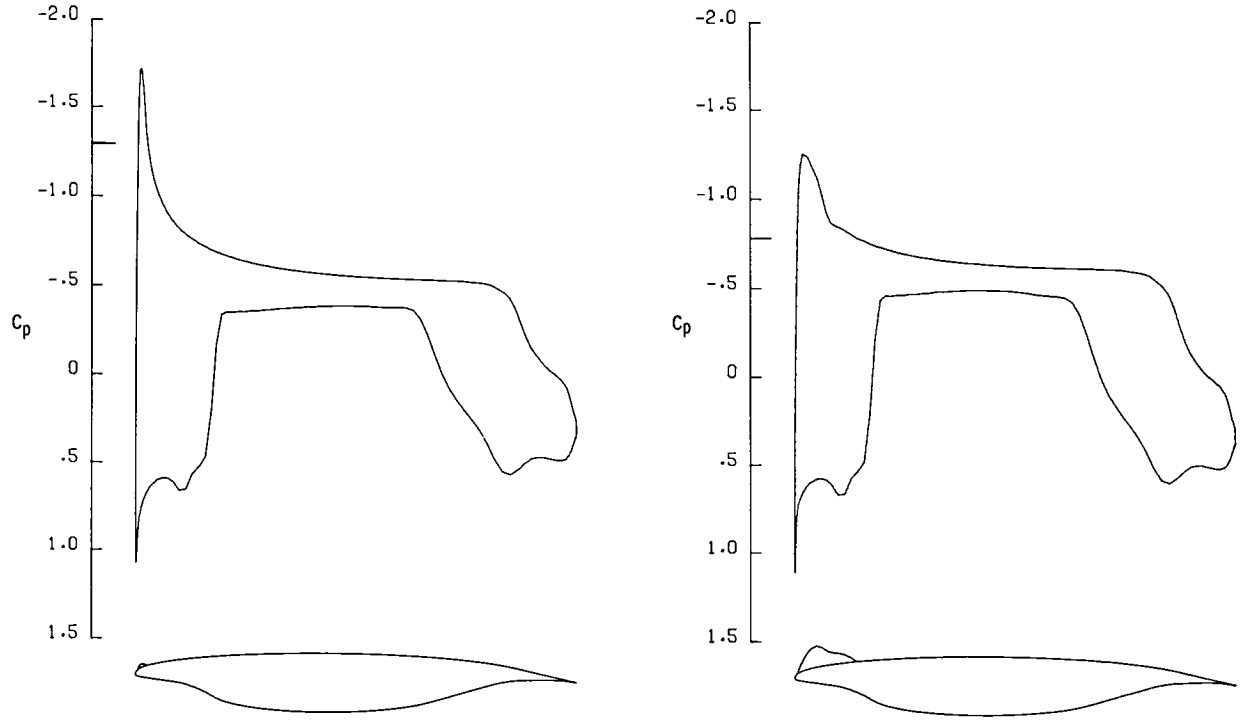

(a) M = 0.600; c_m = -0.096; $c_{d,w}$ = 0.0000.

(b) M = 0.700; c_m = -0.108; $c_{d,w}$ = 0.0000.

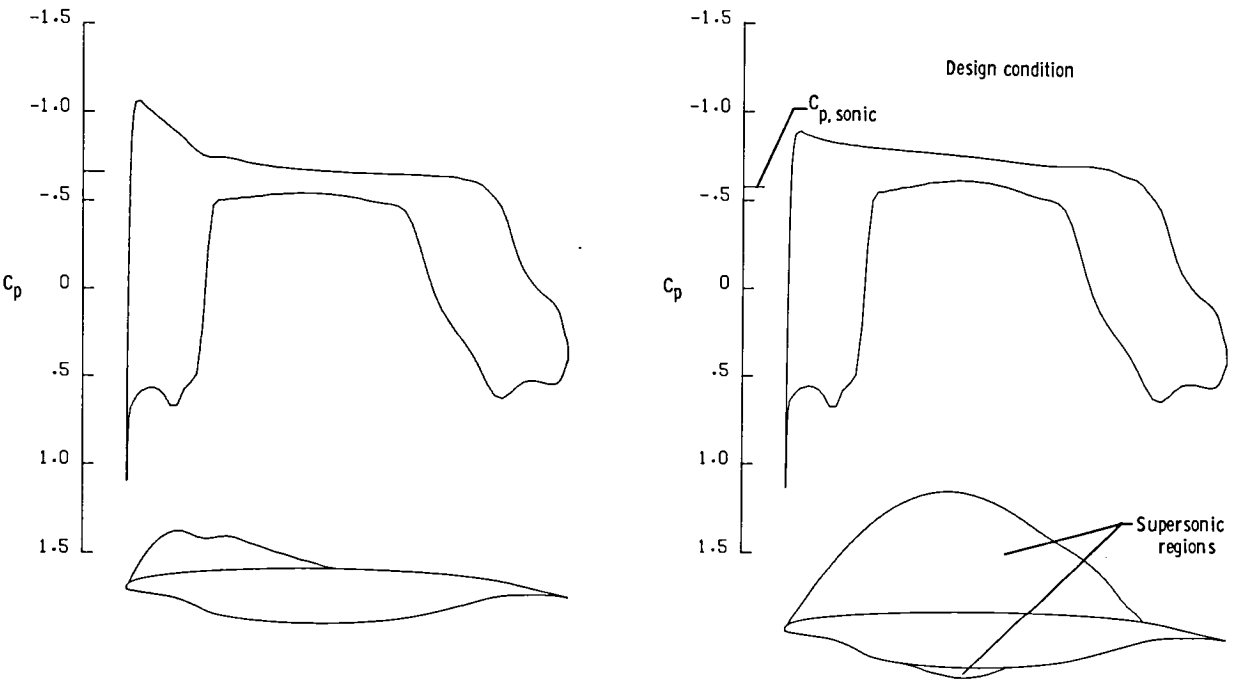

(c) M = 0.730; c_m = -0.115; $c_{d,w}$ = 0.0000.

(d) M = 0.755; c_m = -0.124; $c_{d,w}$ = 0.0000.

Figure 3.- Pressure distributions for airfoil B at M = 0.600 to M = 0.755. c_l = 0.60.

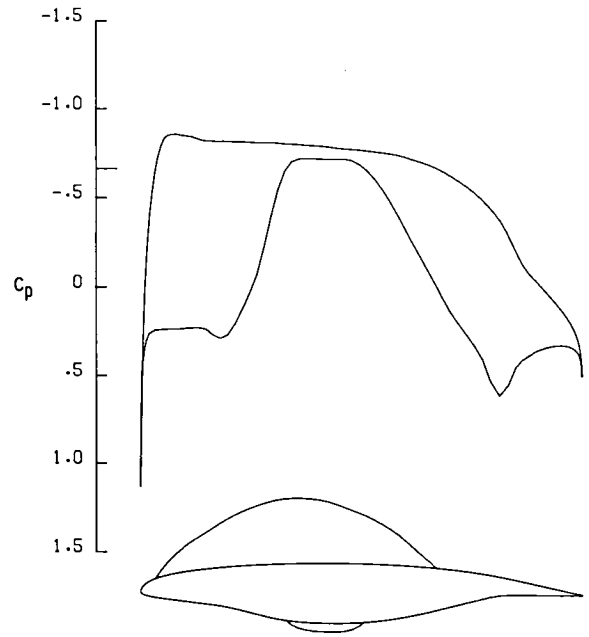

(a) M = 0.730; c_l = 0.55; c_m = -0.103; $c_{d,w}$ = 0.0000.

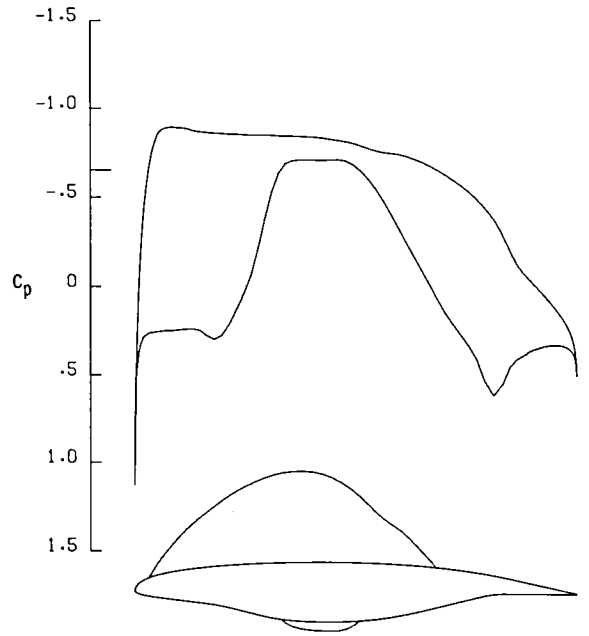

(b) M = 0.733; c_l = 0.58; c_m = -0.105; $c_{d,w}$ = 0.0000.

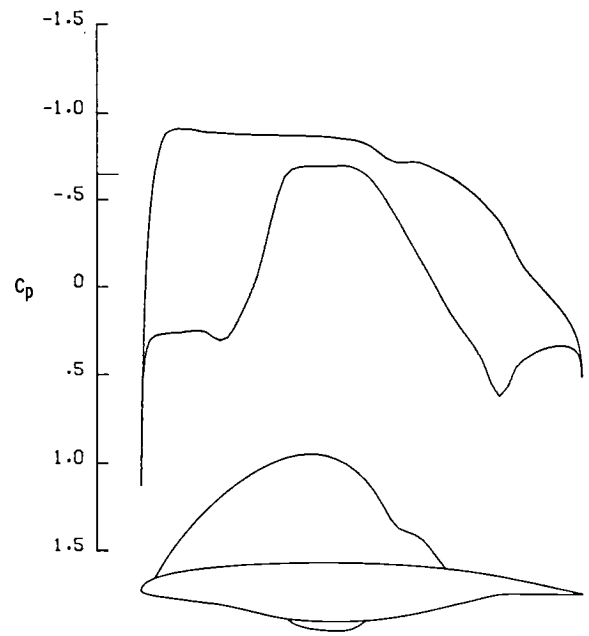

(c) M = 0.735; c_l = 0.60; c_m = -0.106; $c_{d,w}$ = 0.0000.

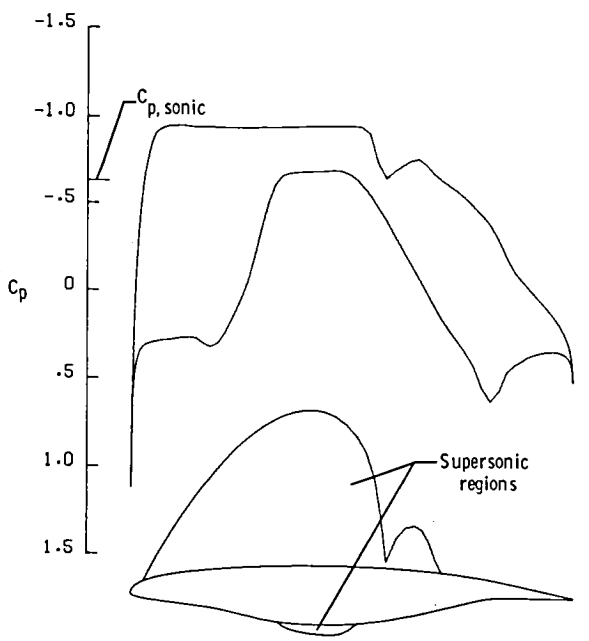

(d) M = 0.740; c_l = 0.65; c_m = -0.111; $c_{d,w}$ = 0.0004.

Figure 4.- Pressure distributions for airfoil A at simultaneously increasing Mach numbers and lift coefficients.

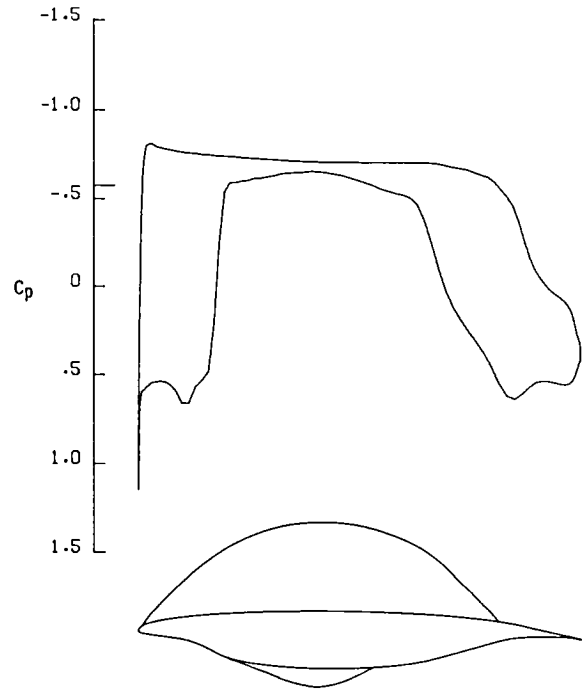

(a) M = 0.755; c_l = 0.55; c_m = -0.122; $c_{d,w}$ = 0.0000.

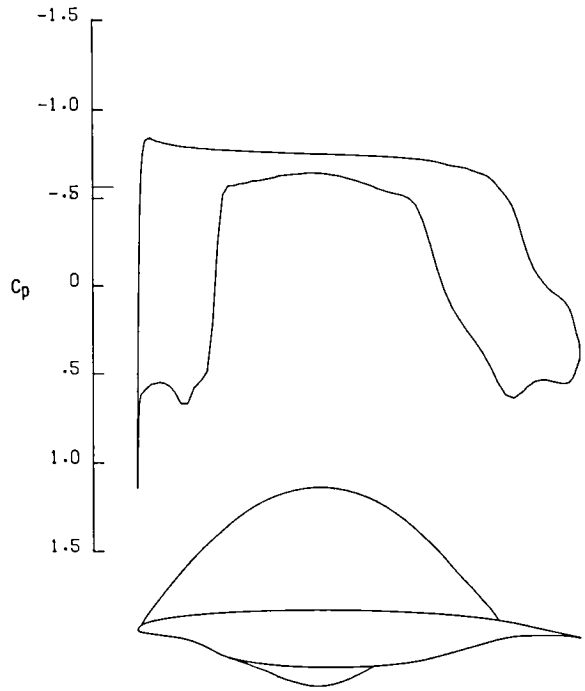

(b) M = 0.758; c_l = 0.58; c_m = -0.125; $c_{d,w}$ = 0.0000.

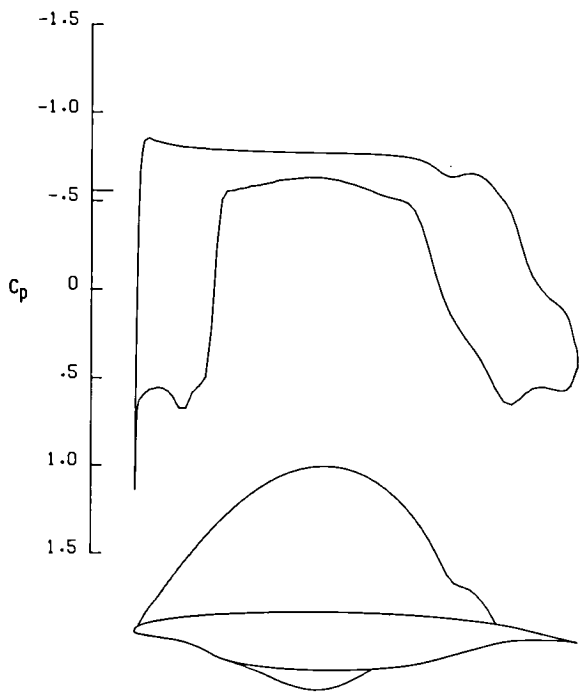

(c) M = 0.760; c_l = 0.60; c_m = -0.127; $c_{d,w}$ = 0.0000.

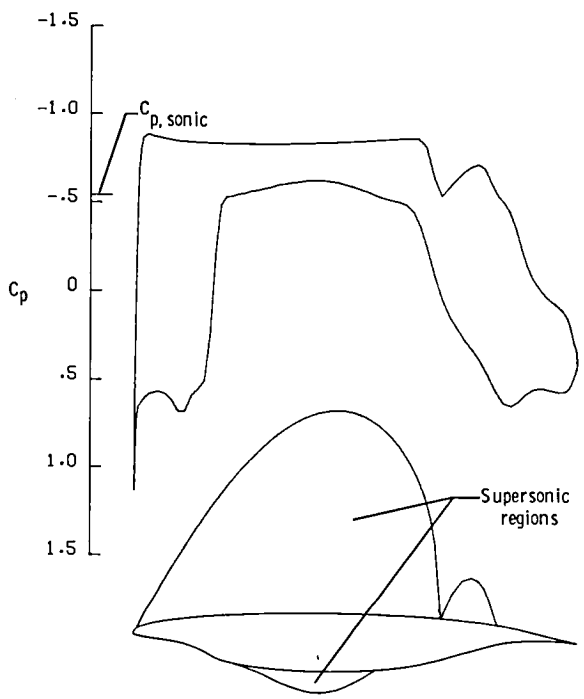

(d) M = 0.765; c_l = 0.65; c_m = -0.134; $c_{d,w}$ = 0.0004.

Figure 5.- Pressure distributions for airfoil B at simultaneously increasing Mach numbers and lift coefficients.

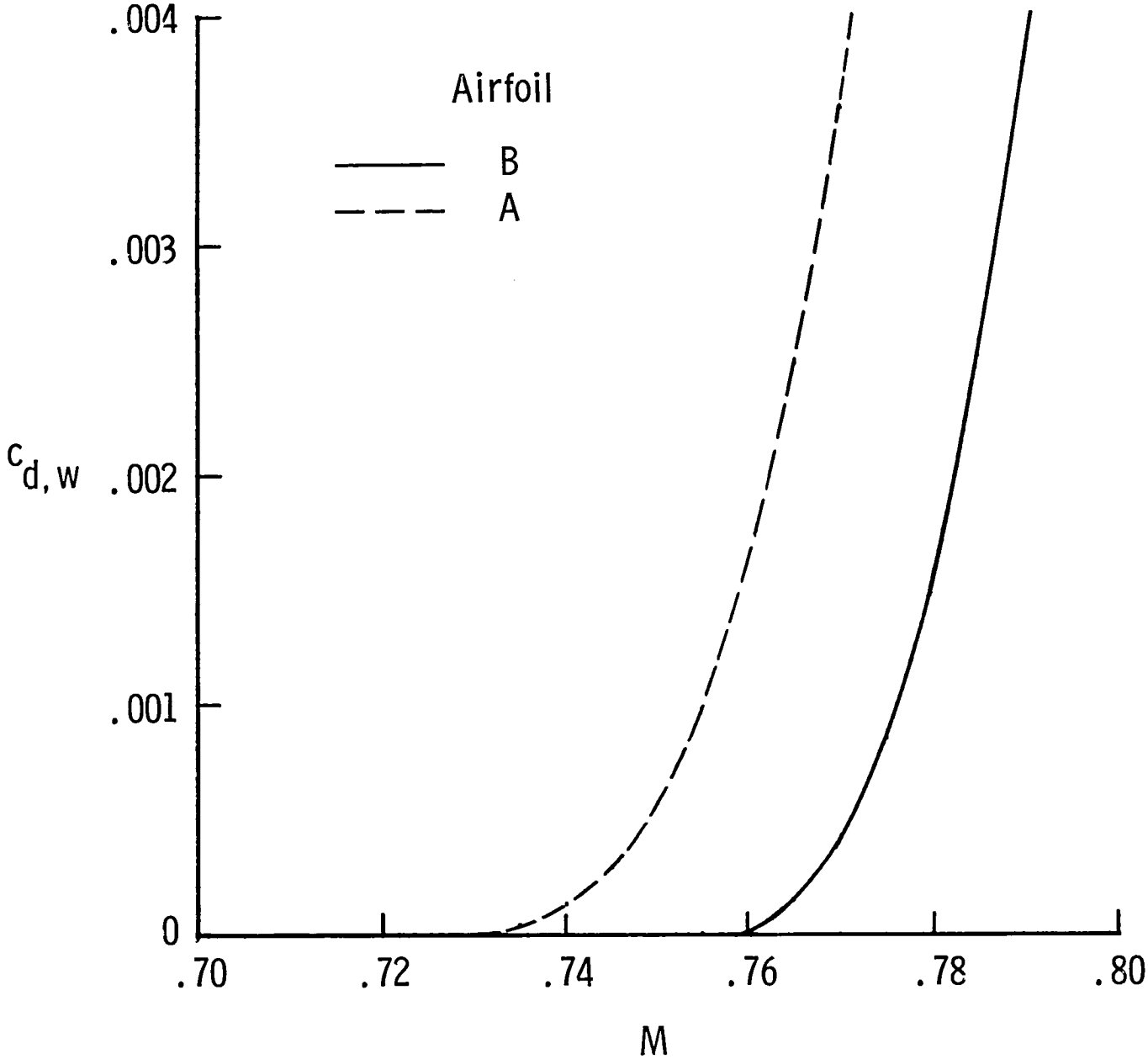

Figure 6.- Comparison of wave drag coefficients for airfoils A and B. $c_l = 0.60$.

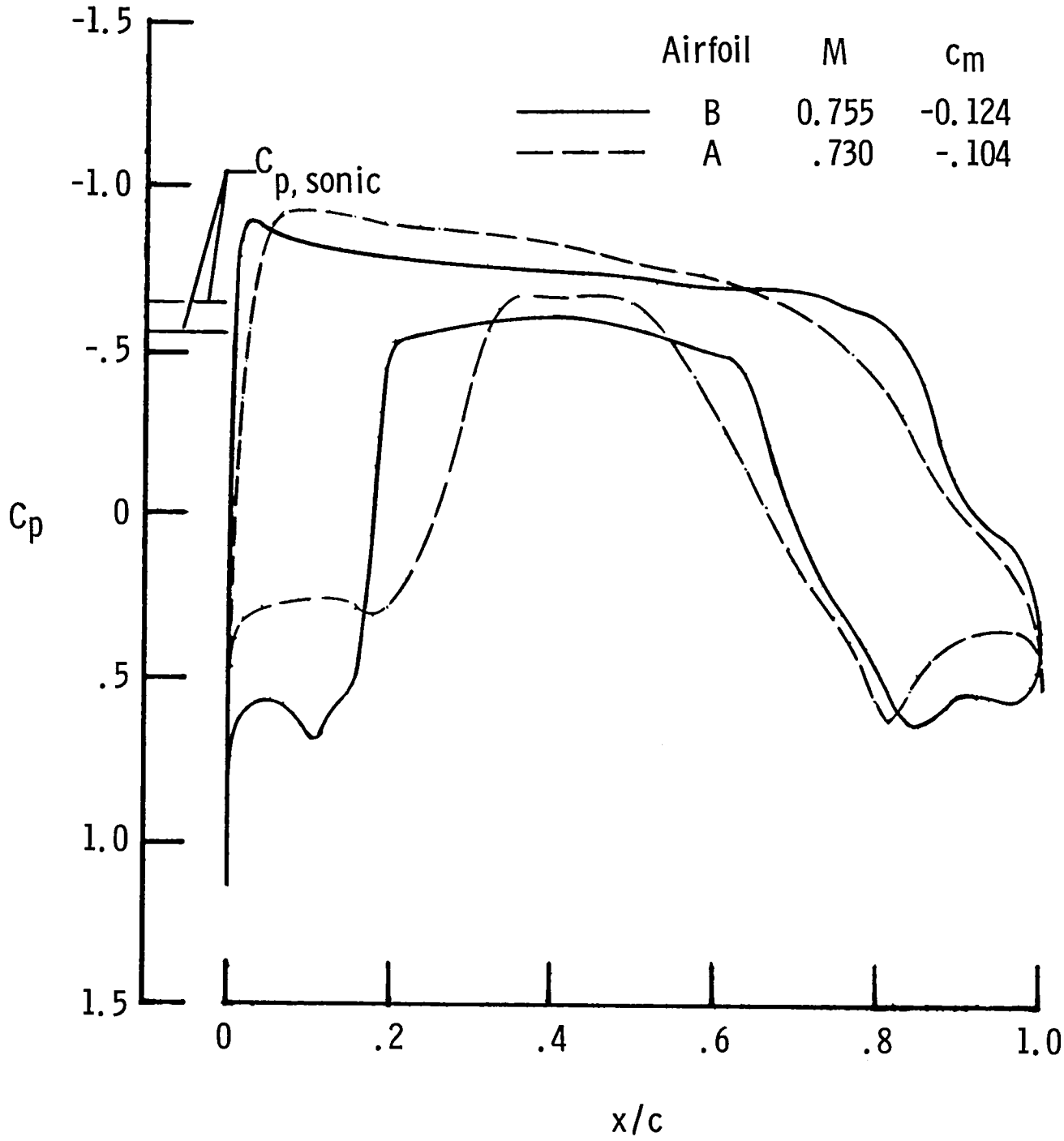

Figure 7.- Comparison of pressure distributions for airfoils A and B at design Mach numbers. $c_l = 0.60$.

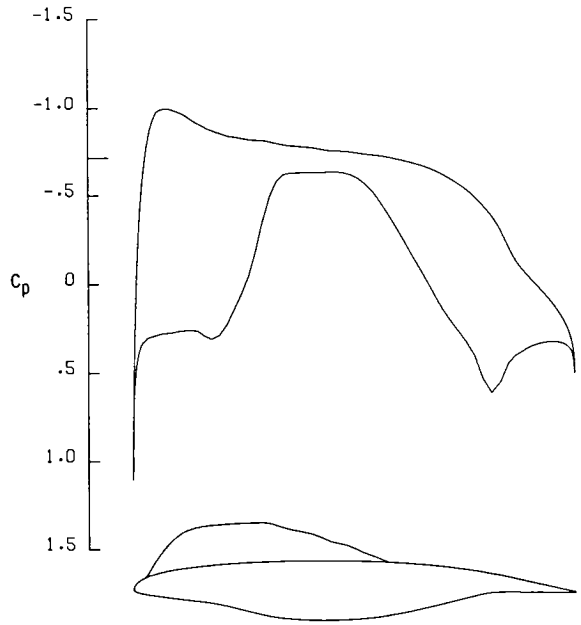

(a) M = 0.715; c_m = -0.100; $c_{d,w}$ = 0.0000.

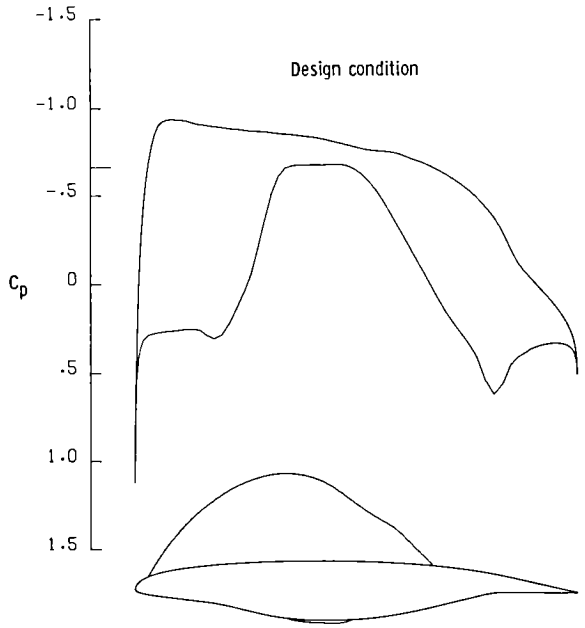

(b) M = 0.730; c_m = -0.104; $c_{d,w}$ = 0.0000.

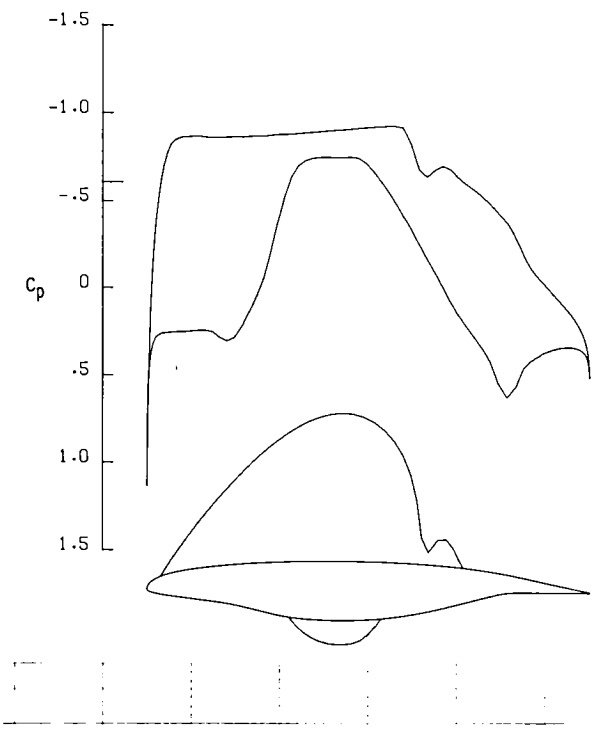

(c) M = 0.745; c_m = -0.111; $c_{d,w}$ = 0.0003.

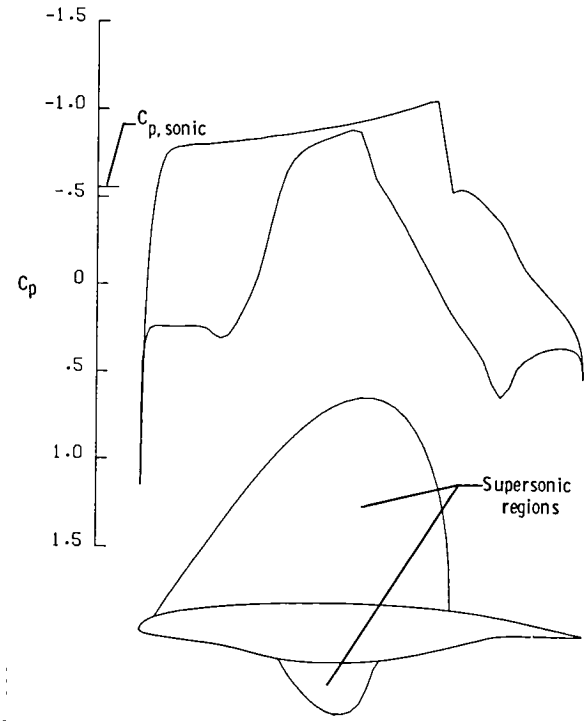

(d) M = 0.760; c_m = -0.124; $c_{d,w}$ = 0.0016.

Figure 8.- Pressure distributions for airfoil A at Mach numbers near the design condition. c_l = 0.60.

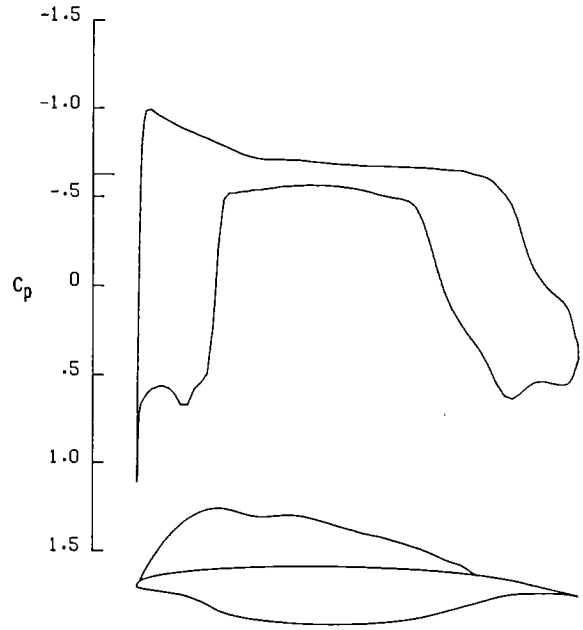

(a) M = 0.740; c_m = -0.118; $c_{d,w}$ = 0.0000.

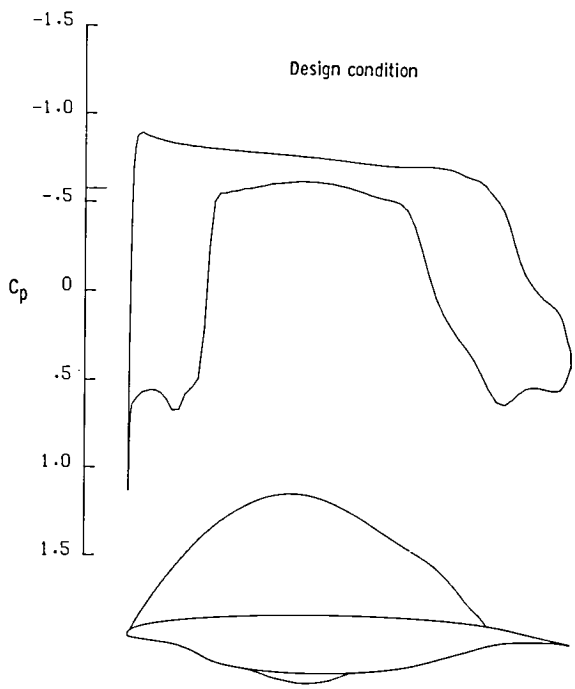

(b) M = 0.755; c_m = -0.124; $c_{d,w}$ = 0.0000.

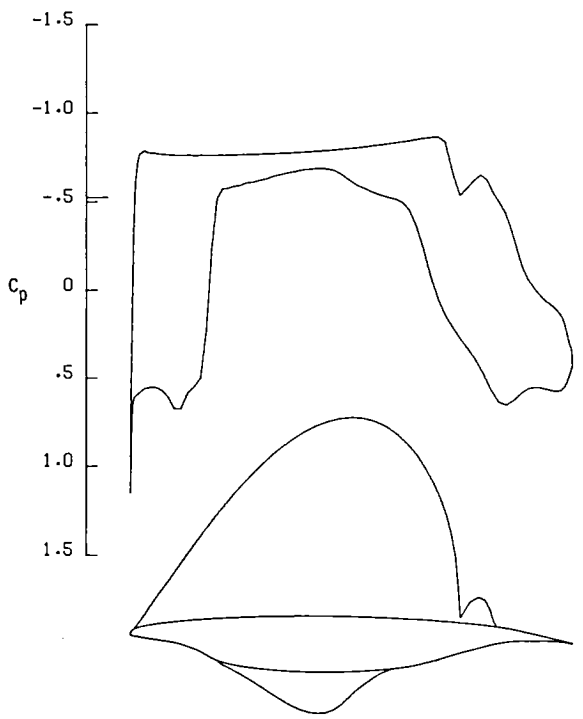

(c) M = 0.770; c_m = -0.135; $c_{d,w}$ = 0.0004.

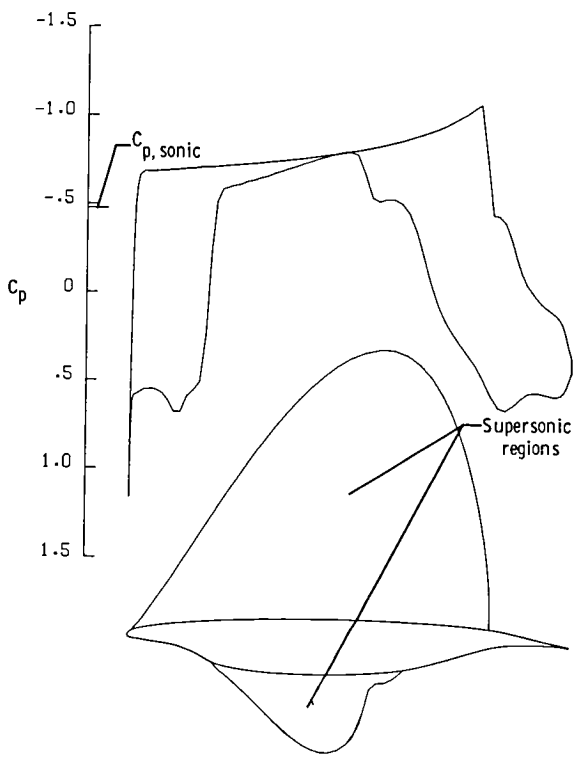

(d) M = 0.785; c_m = -0.153; $c_{d,w}$ = 0.0025.

Figure 9.- Pressure distributions for airfoil B at Mach numbers near the design condition. c_l = 0.60.

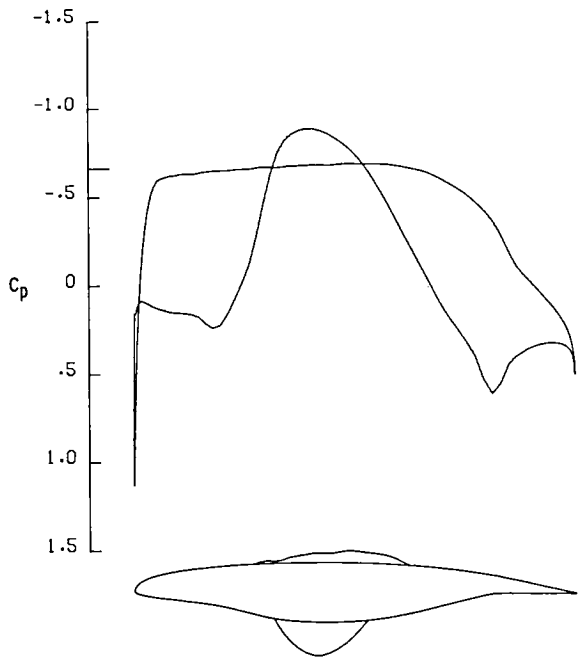

(a) $c_l = 0.40$; $c_m = -0.099$; $c_{d,w} = 0.0000$.

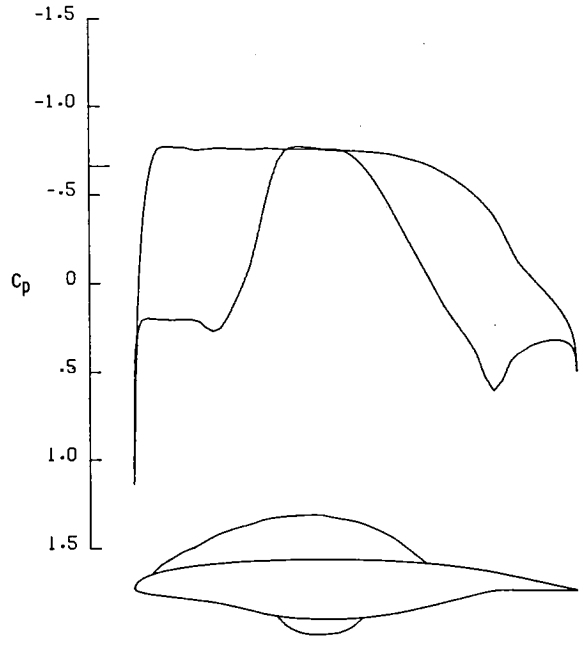

(b) $c_l = 0.50$; $c_m = -0.102$; $c_{d,w} = 0.0000$.

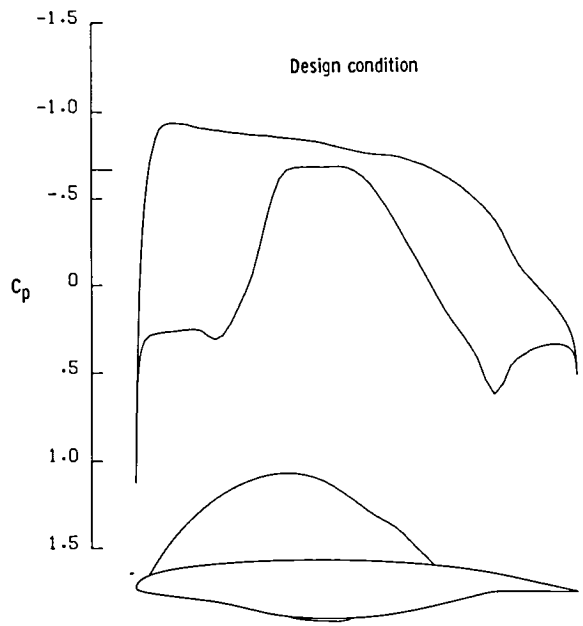

(c) $c_l = 0.60$; $c_m = -0.104$; $c_{d,w} = 0.0000$.

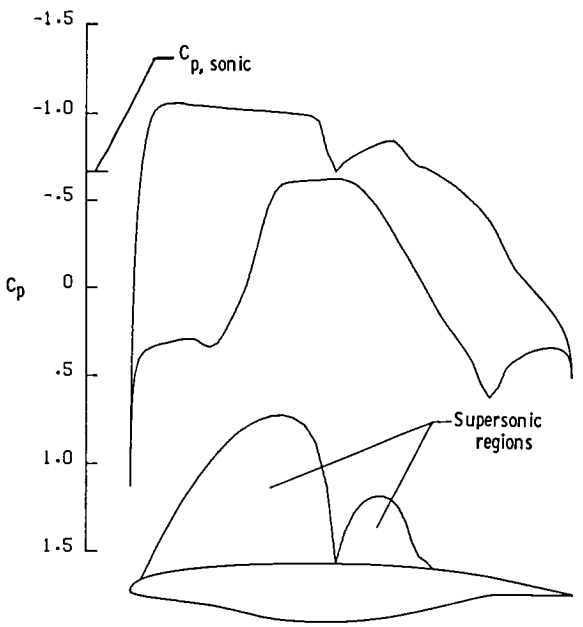

(d) $c_l = 0.70$; $c_m = -0.108$; $c_{d,w} = 0.0004$.

Figure 10.- Pressure distributions for airfoil A at $c_l = 0.40$ to $c_l = 0.70$. $M = 0.730$.

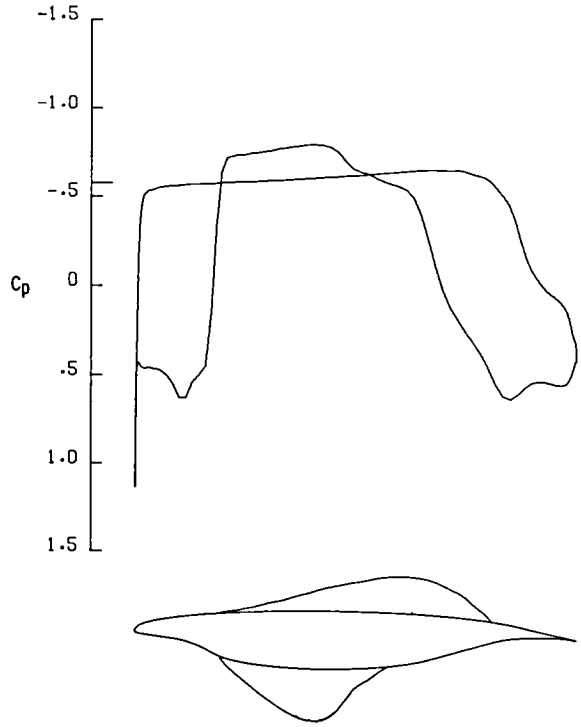

(a) $c_l = 0.40$; $c_m = -0.117$; $c_{d,w} = 0.0000$.

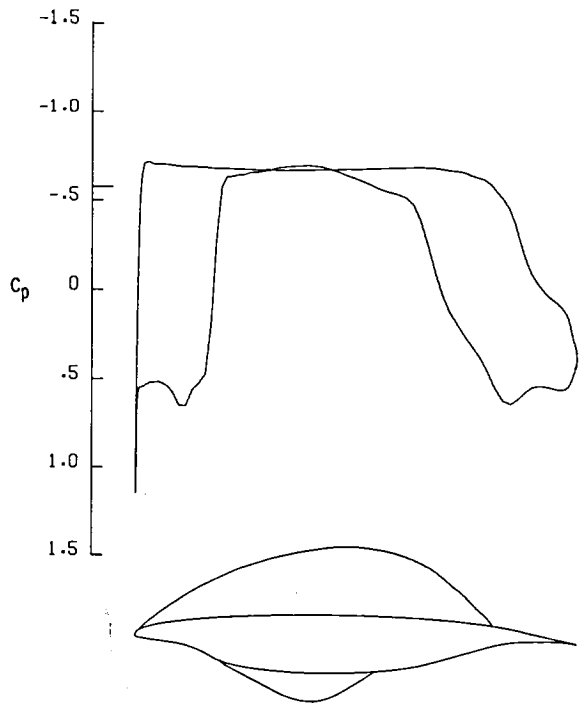

(b) $c_l = 0.50$; $c_m = -0.121$; $c_{d,w} = 0.0000$.

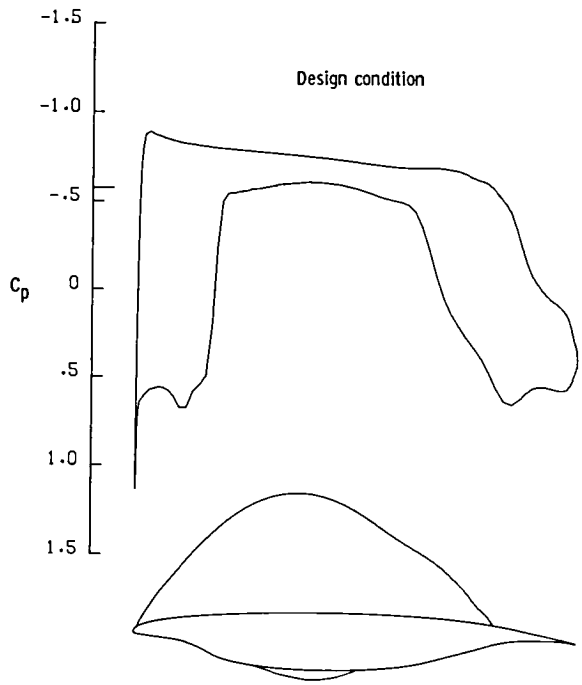

(c) $c_l = 0.60$; $c_m = -0.124$; $c_{d,w} = 0.0000$.

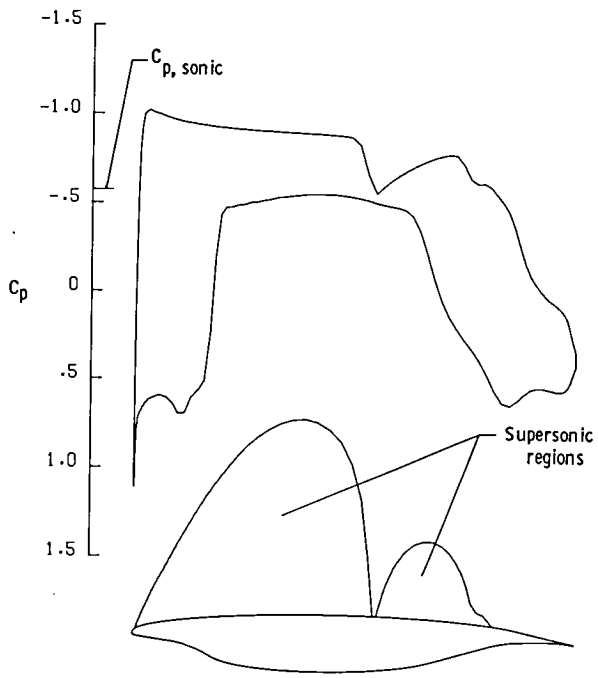

(d) $c_l = 0.70$; $c_m = -0.128$; $c_{d,w} = 0.0005$.

Figure 11.- Pressure distributions for airfoil B at $c_l = 0.40$ to $c_l = 0.70$. $M = 0.755$.

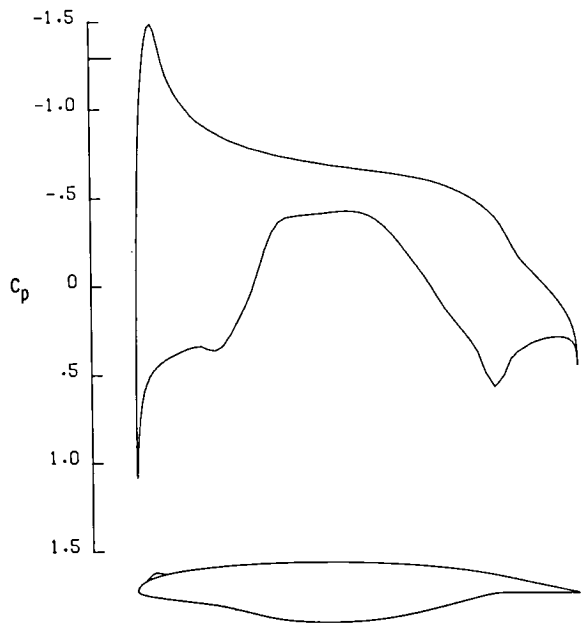

(a) M = 0.600; c_m = -0.086; $c_{d,w}$ = 0.0000.

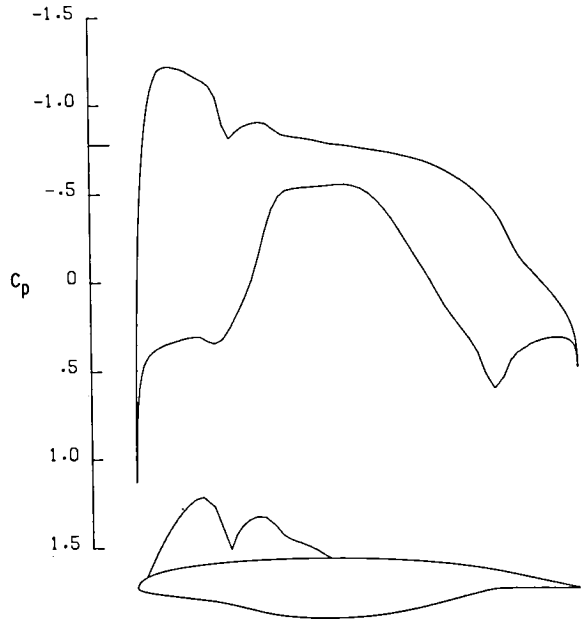

(b) M = 0.700; c_m = -0.099; $c_{d,w}$ = 0.0001.

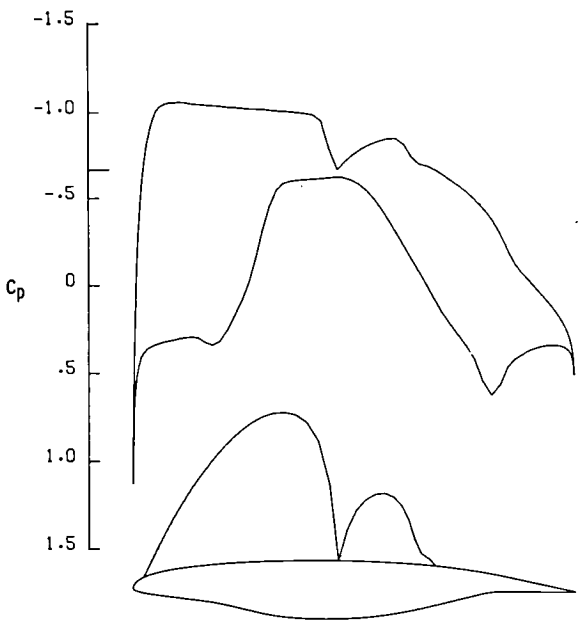

(c) M = 0.730; c_m = -0.108; $c_{d,w}$ = 0.0004.

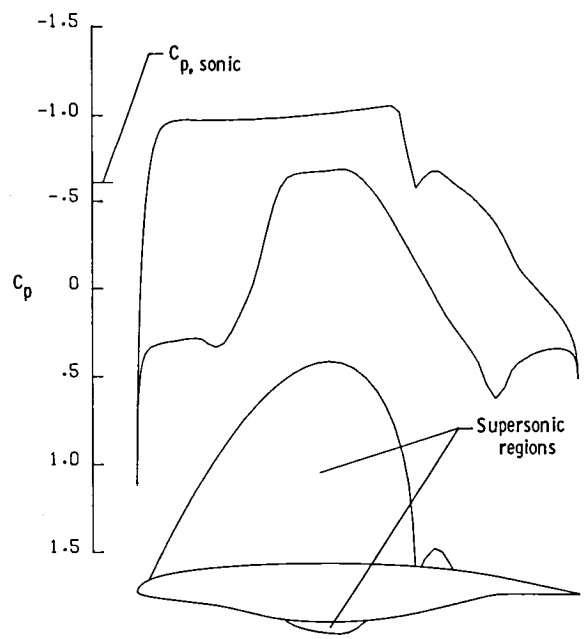

(d) M = 0.745; c_m = -0.118; $c_{d,w}$ = 0.0011.

Figure 12.- Pressure distributions for airfoil A at M = 0.600 to M = 0.745. c_l = 0.70.

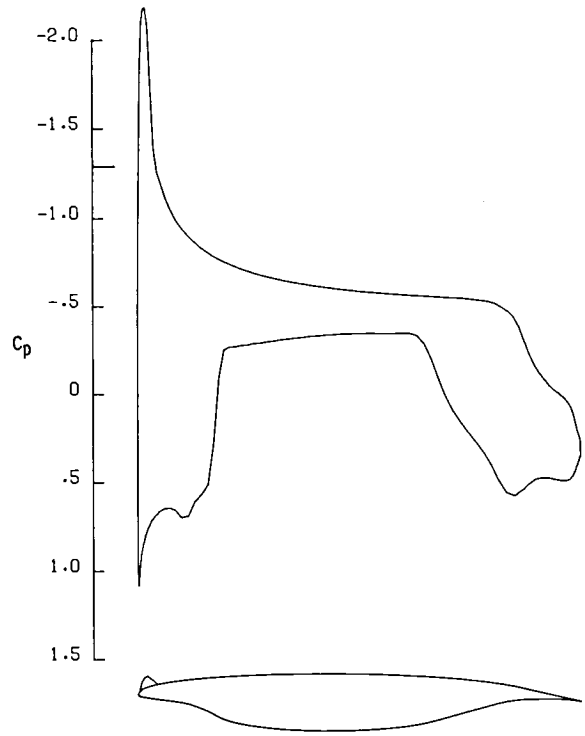

(a) M = 0.600; c_m = -0.096; $c_{d,w}$ = 0.0000.

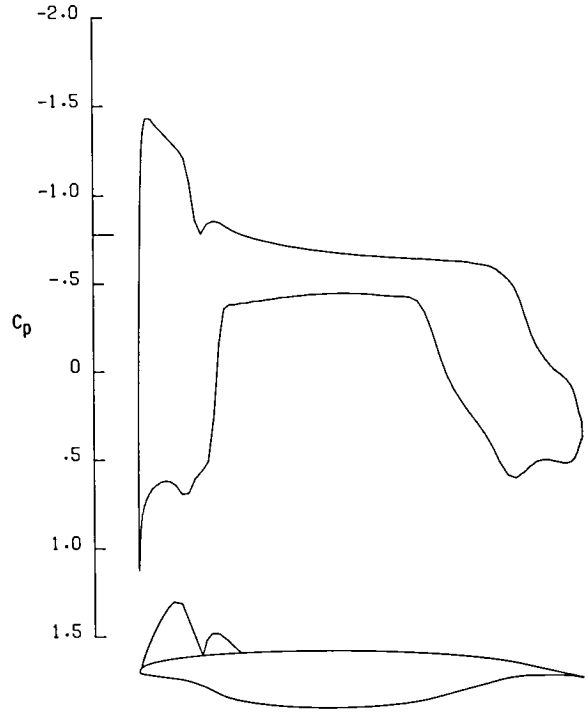

(b) M = 0.700; c_m = -0.109; $c_{d,w}$ = 0.0002.

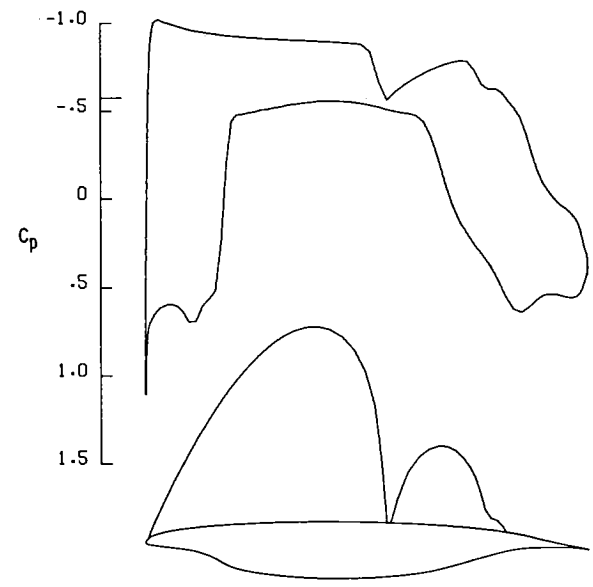

(c) M = 0.755; c_m = -0.128; $c_{d,w}$ = 0.0005.

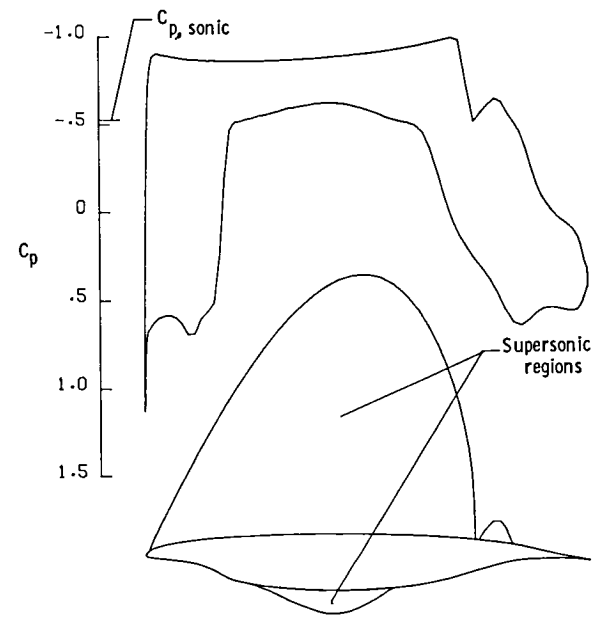

(d) M = 0.770; c_m = -0.144; $c_{d,w}$ = 0.0014.

Figure 13.- Pressure distributions for airfoil B at M = 0.600 to M = 0.770. c_l = 0.70.

1. Report No.	2. Government Accession No.	3. Recipient's Catalog No.
NASA TM-84657		

4. Title and Subtitle	5. Report Date
INVISCID ANALYSIS OF TWO SUPERCRITICAL LAMINAR-FLOW-CONTROL AIRFOILS AT DESIGN AND OFF-DESIGN CONDITIONS	June 1983
	6. Performing Organization Code 505-31-23-06

7. Author(s)	8. Performing Organization Report No.
Dennis O. Allison	L-15571
	10. Work Unit No.

9. Performing Organization Name and Address	11. Contract or Grant No.
NASA Langley Research Center Hampton, VA 23665	
	13. Type of Report and Period Covered Technical Memorandum

12. Sponsoring Agency Name and Address	14. Sponsoring Agency Code
National Aeronautics and Space Administration Washington, DC 20546	

15. Supplementary Notes

16. Abstract

Inviscid transonic flow results are provided at design and off-design conditions for two supercritical laminar-flow-control airfoils. The newer airfoil, with its lower suction requirements for full-chord laminar flow, has a higher design Mach number, steeper pressure gradients, a more positive pressure level in the forward region of the lower surface, and a recovery to a less positive pressure at the trailing edge. The two-dimensional design Mach numbers for the two airfoils are 0.755 and 0.730 at a common design lift coefficient of 0.60, and their thickness-to-chord ratios are 0.131 and 0.135, respectively. Off-design shock-formation characteristics are similar for the two airfoils over a range of Mach numbers between 0.6 and 0.8 and lift coefficients from 0.4 to 0.7. The newer airfoil is similar to the one used in a large-chord swept-model experiment designed for the Langley 8-Foot Transonic Pressure Tunnel.

17. Key Words (Suggested by Author(s))	18. Distribution Statement
Airfoils Laminar flow control Supercritical Pressure distributions Swept wings	~~[redacted] Distribution~~ Subject Category 02

19. Security Classif. (of this report)	20. Security Classif. (of this page)	21. No. of Pages	22. Price
Unclassified	Unclassified	20	

Available: NASA's Industrial Applications Centers

NASA-Langley, 1983